Application concepts for complementary micro-pneumatic devices and circuits

Albert K. Henning*
Aquarian Microsystems, 199 Heather Lane, Palo Alto, CA 94303-3002

ABSTRACT

Previously, we proposed novel microvalve structures, amenable to bulk micromachining, which demonstrated fully complementary behavior. Two distinct microvalves were devised, one analogous to the p-MOSFET, and the other analogous to the n-MOSFET found in complementary MOSFET devices and circuits. Ring oscillator behavior based on *digital* NOR logic gates was described, for both micro-pneumatics (based on compressible gas flow) and micro-hydraulics (based on incompressible liquid flow). In this work, micro-pneumatic *analog* circuits are described, based on the previously-described complementary digital pneumatic microvalve devices. In particular, a micro-pneumatic operational amplifier is described and simulated in detail. Also, prospects for energy harvesting or scavenging based on micro-pneumatic circuits are discussed.

Keywords: micropneumatic logic, pneumatic operation amplifier, pneumatic energy harvesting, energy scavenging, analog micropneumatic circuits, pneumatic rectifier, micro-pump

LIST OF VARIABLES

$\dot{m}$	Mass flow (usually in sccm, normalized to 273 K and 1 atm)
P_c	Control pressure
P_i	Inlet pressure
P_o	Outlet pressure
P_t	Threshold pressure
γ	Ratio of specific heats, c_p/c_v
α	$= \sqrt{\gamma\left(\frac{2}{1+\gamma}\right)^{\frac{\gamma+1}{\gamma-1}}}$
δ	$= \sqrt{\frac{4\gamma}{(\gamma+1)(\gamma-1)}}$
R	Gas constant in $p = \rho RT$ (8314 m^2/K-sec^2 divided by molecular weight)
E	Young's modulus for the membrane material
A_s, B_s	Deflection coefficients for the membrane, related to membrane stroke
D	Microvalve inlet diameter
h	Microvalve membrane thickness
a	Microvalve membrane length (of one side)
W	Microvalve seat perimeter length (usually 4*D)
z	Microvalve membrane-to-inlet gap
z_0	Microvalve membrane-to-inlet gap at zero stroke
s	Microvalve membrane stroke
A_{eff}	Microvalve effective flow area
C_d	Microvalve inlet coefficient of discharge
C_v	Microvalve coefficient of flow
ρ	Density of incompressible liquid

Microfluidics, BioMEMS, and Medical Microsystems VI, edited by Wanjun Wang, Claude Vauchier,
Proc. of SPIE Vol. 6886, 68860F, (2008) · 0277-786X/08/$18 · doi: 10.1117/12.771200

1. INTRODUCTION

Systems of devices which process information (that is, energy) transform an input excitation into an output result using flow of a working fluid.

There are many working fluids found in information processing systems, if 'information processing' is taken in its broadest sense. In our modern world, filled with computers and computer applications, electronic devices use the flow of a compressible electron or hole gas, in order to transmit or process information. But electrons are not the only particles which can communicate information. Electrons communicate charge information. But photons communicate light, or optical, information. Phonons communicate heat, or thermal, information. And atoms or molecules communicate information about species and mass.

Systems based on the flow of electrons are called 'electronic'. In such systems, the charge elements of the electron gas obey Fermi-Dirac statistics: each element of the gas has a different state, or set of quantum numbers. For phonon (phononic) and photon (photonic) systems, and for superconducting systems, the particles of the working fluid obey Bose-Einstein statistics: each element of the ensemble has the same state, or set of quantum numbers.

For systems where the working fluid is comprised of uncharged atoms or molecules, two types of systems occur. When the thermodynamic state of the working fluid is a gas, then it is compressible, and systems based on such working fluids are called 'pneumatic'. On the other hand, when the thermodynamic state of the working fluid is a liquid, then it is largely incompressible, and systems based on such working fluids are called 'hydraulic.'

In *primary* information processing systems, the input excitation and the output result have the same form. For instance, in electronic integrated circuits, the input and output are both voltages. Similarly, in micropneumatic or microhydraulic circuits, the input and output are both pressures. In *secondary* information processing systems, the input excitation and output result have different forms. For instance, in digital mirror devices, an electrical input is transformed into a mechanical output (to control the mirror position). Similarly, in some microfluidic systems, a pneumatic input is transformed into a hydraulic output [1, 2]. In other such systems, hydraulic or pneumatic inputs are transformed into optical outputs [3]. Other secondary transform modalities include electric-to-fluidic (either pneumatic or hydraulic) [4-6], and electric-to-chemical [7, 8].

In the realm of *primary* information processing systems using micropneumatic circuits, several digital and analog approaches have been taken. Micropneumatic valves using silicon and glass have been described by Takao, *et al.* [9, 10]. Using bulk micromachining, these devices were constructed in a lateral fashion, with flow over a barrier constricted by a movable diaphragm seating against this barrier. Analogous to MOSFET integrated circuit technologies, enhancement-enhancement and enhancement-depletion structures were utilized to realize both digital (NOR gate) and analog (small-signal amplification) behavior. Related active-gate-passive-load work appeared earlier, in the form of a high-precision mass-flow controller for semiconductor processing applications [11]. This approach is limited by two attributes. First, the lateral nature of the underlying devices creates parasitic leakage paths. Second, only one form of device is available, so that realization of, for instance, a NOR gate requires a passive, and not active, load in the flow circuit. As is well-known from integrated circuit technologies, circuits based on passive loads tend to be slower, and always consume more power (that is, the working fluid is always moving) in comparison to fully-active circuits.

Another approach has been based on the use of glass and PDMS [12-14], expanding on the use of these materials in simple valve structures in order to realize highly integrated lab-on-a-chip products [1, 2]. This approach has focused on digital logic, through the realization of AND, OR, NOR, NAND, XOR, and ripple-carry adder structures. As the materials are simple, while the resulting structures are complex, this approach is attractive from a system-level standpoint. On the other hand, as with the technology of Refs. 3 and 4, the device elements in this technology consume power continuously, in order to preserve any particular logic state. And, once the input excitation is removed, storage of logic information or preservation of a particular logic state lasts for only a brief period of time, because of this continuous consumption of power.

In this work, therefore, we focus on fully complementary devices [15, 16] related to *primary* information processing systems based on micropneumatic valves. Whereas our previous efforts described digital manifestations of these devices, here we will focus on analog circuits. In particular, we will describe operational amplifiers, pressure rectifiers (pumps), and pneumatic energy harvesting systems.

2. COMPLEMENTARY MICROPNEUMATIC DEVICES

To begin, we reiterate the qualitative and quantitative description of complementary micropneumatic devices.

Figure 1 portrays a normally-open microvalve. The microvalve has a flexible membrane, whose position z relative to the valve seat is controlled by the difference between control pressure P_c, and the inlet and outlet pressures P_i and P_o. The work in Ref. 17 describes the full behavior of microvalve flow, under sonic and subsonic conditions, while accounting for the additional non-linearities of flow as the valve first opens. The membrane deflection s from the equilibrium position z_0 is essential to the control of flow. The membrane thickness is h, the area is a, and the Young's modulus is E. γ is the specific heat ratio for the compressible gas. If an 'edgeless' microvalve is used, then most of the complications associated with inhomogeneous membrane pressure loading (in Refs. 9 and 10) disappear.

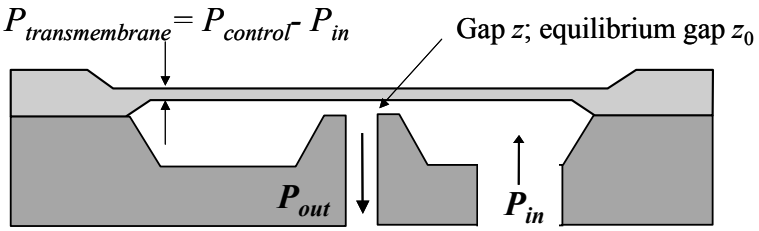

Figure 1: Schematic of a typical normally-open microvalve.

2.1 Normally-closed valve

Figure 2 shows the first basic micro-pneumatic logic element [15]. The central boss, and the construction process, provide an initial tension, which must be overcome by a threshold control pressure before the valve opens. The microvalve is therefore normally-closed, and the transmembrane pressure P_i-P_c must exceed a threshold value P_t before the valve permits the flow of the working fluid. The quantitative details of the relationship between the threshold pressure and the structural parameters of the valve are found in Ref. 17, and reiterated in Equation (1), below.

'Edgeless' structures distinguish themselves from the enhancement-depletion devices in Refs. 9 and 10. They enable leak-free behavior when their individual elements are OFF, by placing a smooth membrane against a smooth valve seat. Alternatively, an elastomeric material can be embodied in the valve seat or the membrane boss, in order to retain minimum or zero leakage in the OFF state.

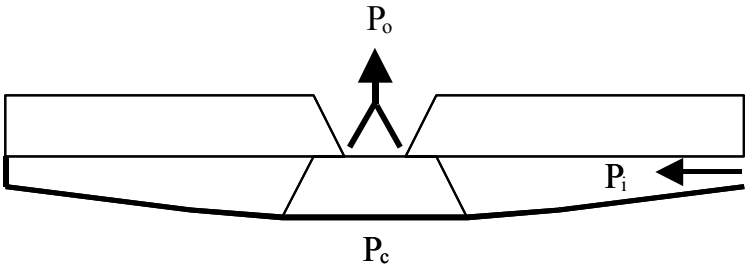

Figure 2: Cross-section of a normally-closed microvalve.

2.2 Normally-closed poppet valve

Figure 3 shows the second basic micro-pneumatic logic element [15]. Here, the central boss is replaced by a poppet structure. The microvalve is therefore also normally-closed, but now the transmembrane pressure P_c-P_i must exceed a threshold value P_t before the valve permits the flow of the working fluid. That is: the sign of transmembrane pressure which opens the valve of Figure 3 is the opposite of the related pressure which opens the valve of Figure 2. This distinction is crucial to the realization of complementary, digital or analog micro-pneumatic circuits. The quantitative details of the relationship between the threshold pressure and the structural parameters of the valve are found in Ref. 17, and are reiterated in Equations (1), below.

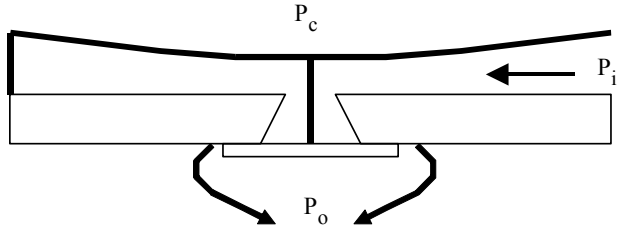

Figure 3: Cross-section of a normally-closed poppet microvalve. Flow directions are indicated by the arrows.

2.3 Micro-pneumatic models (compressible gases)

Equations 1 relate the pneumatic boundary conditions, mechanical behavior of a microvalve membrane, and the microvalve flow model for the normally-closed poppet microvalve [17]. Though not elaborated in this work, the sonic and subsonic flow equations have close analogies to, respectively, the saturation and linear equations for electron flow in MOSFETs. Figures 4 and 5 show the results of applying this model to the structure of Fig. 3, using the model (structural, material, and boundary condition) parameters shown in the figure. The membrane is silicon, 4.5 mm square and 50 μm thick.

$$z = z_0 - s \qquad P_t \equiv EA_s \frac{z_0 h^3}{a^4} \qquad \frac{(P_c - P_i)a^4}{Eh^4} = A_s \frac{s}{h} + B_s \frac{s^3}{h^3} \Rightarrow \frac{P_{ci} a^4}{Eh^4} \cong A_s \frac{s}{h}$$

$$A_{eff} = Wz = W(z_0 - s) = Wa \frac{a^3}{h^3} \frac{1}{A_s E}(P_t - P_{ci}) \qquad (1)$$

$$\dot{m}_{sonic} \equiv \dot{m}_{sonic}(P_o, P_i, P_c) = C_d C_v \frac{\alpha(\gamma)}{\sqrt{RT}} Wa \frac{a^3}{h^3} \frac{1}{A_s E}(P_t - P_{ci}) P_o$$

$$\dot{m}_{subsonic} \equiv \dot{m}_{subsonic}(P_o, P_i, P_c) = C_d C_v \frac{\delta(\gamma)}{\sqrt{RT}} Wa \frac{a^3}{h^3} \frac{1}{A_s E}(P_t - P_{ci}) P_o \left(\frac{P_i}{P_o}\right)^{\frac{\gamma+1}{2\gamma}} \sqrt{\left(\frac{P_o}{P_i}\right)^{\frac{\gamma-1}{\gamma}} - 1}$$

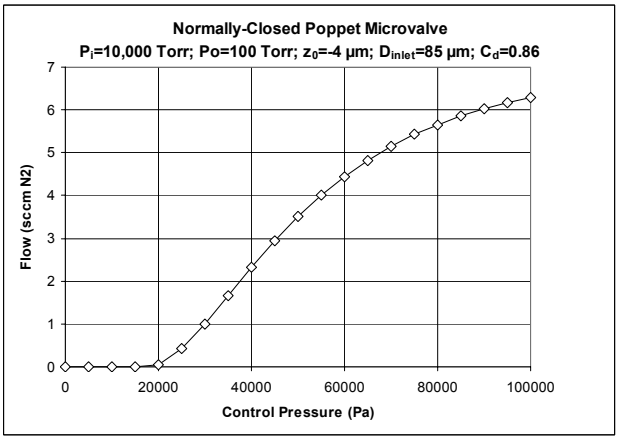

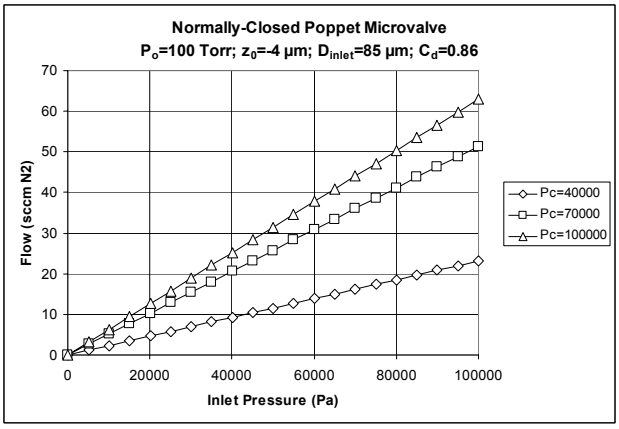

Left: Figure 4: Control pressure characteristic for a normally-closed poppet microvalve. The gas is nitrogen, and the gas stagnant temperature is 298 K. Right: Figure 5: Inlet pressure characteristic for the normally-closed poppet microvalve of Figure 3.

3. COMPLEMENTARY MICROPNEUMATIC ANALOG CIRCUITS

Using the basic micro-pneumatic device elements (valves) of Figures 2 and 3 as fundamental building blocks, digital micro-pneumatic devices, such as NOR and NAND gates, were described previously [15, 16]. In this section, we describe a number of complementary, micro-pneumatic analog circuits, and the performance of examples of such circuits based on the model of Equations (1).

3.1 Differential Operational Amplifier

Figure 6 depicts schematically the essential components of a differential operational amplifier, based upon a compressible gas as the working fluid. The devices labeled PU_x are the normally-closed valve of Figure 2, while those labeled PD_x are the normally-closed valve of Figure 3. 'PU' is thus taken to mean 'pull-up', while 'PD' means 'pull-down', in the sense common to MOSFET integrated circuit design. The open loop gain of a differential operational amplifier is defined to be $G=P_{OUT}/(P_{IN,HI}-P_{IN,LO})$. Because the devices in Figures 2 and 3 are asymmetrical (unlike the devices of Refs. 9 and 10), the filled triangles in the device icons indicate the preferred direction of mass flow.

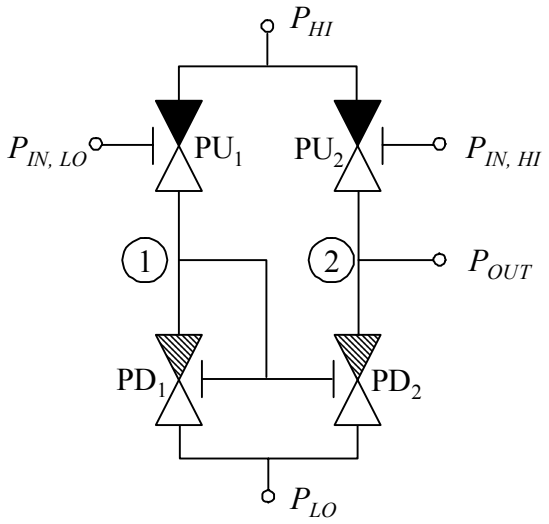

Figure 6: Schematic diagram of the essential portion of a complementary, micro-pneumatic differential operational amplifier.

The state equations used to solve this circuit and determine both its transient and steady-state performance are given in Equations (2). There are two independent nodes in the system, labeled 1 and 2 in Figure 6. A control volume drawn around each node allows Equations (2) to be written: the amount of mass stored at each node per unit time is equal to the difference between the mass flowing in (through the pull-up devices) and the mass flowing out (through the pull-down devices). Because the working fluid is compressible, and because the volumes at each node are fixed (equal to 10^{-9} m^{-3}), the mass stored per unit time can be found from the time derivative of the ideal gas equation, $P_nV_n=m_nRT$.

$$\begin{aligned}
\frac{dm_1}{dt} &= \dot{m}_{PU_1} - \dot{m}_{PD_1} = \frac{V_1}{RT}\frac{dP_1}{dt} \\
&= \dot{m}_{PU_1}\left(P_{HI}, P_1, P_{IN,LO}\right) - \dot{m}_{PD_1}\left(P_1, P_{LO}, P_1\right) \\
\frac{dm_2}{dt} &= \dot{m}_{PU_2} - \dot{m}_{PD_2} = \frac{V_2}{RT}\frac{dP_2}{dt} \\
&= \dot{m}_{PU_2}\left(P_{HI}, P_2, P_{IN,HI}\right) - \dot{m}_{PD_2}\left(P_2, P_{LO}, P_1\right)
\end{aligned} \qquad (2)$$

The results are shown in Figure 7, for a 'standard' microvalve size (commensurate with the state of the present art), and a scaled microvalve technology. As with electronic operational amplifiers based on CMOS technology, the open loop gain is highest for the smallest differential inputs, and decreases according to a power law as the magnitude of the differential input increases. For the standard and scaled designs examined here, impressive open loop gains are achieved, which suggests high-performance pneumatic differential amplifiers can be realized from this complementary microvalve technology. For the standard technology, across all values of differential input, the mass flow of nitrogen is approximately 31 sccm (6.1×10^{-7} kg/sec); for the scaled technology, the nitrogen mass flow is only 5.75×10^{-4} sccm (1.14×10^{-11} kg/sec).

Differential operational amplifiers are characterized in terms of their cut-off frequency. For the standard microvalve technology, with a volume associated with each node in the circuit of 10^{-9} m^{-3} (that is, a cube 1 mm on a side), the cut-off frequency is 1500 Hz, and does not roll-off until the differential input dP exceeds 10,000 Pa. Cut-off frequency is determined by examining the transient response as the system moves from one dP state to another, according to Equations (2). As noted from Equations (2), the cut-off frequency is inversely proportional to the size of the capacitive storage volume associated with the output node of the circuit. For the scaled microvalve technology, with a nodal volume of 10^{-15} m^{-3}, or a cube 10 µm on a side, the cut-off frequency is calculated to be approximately 1.7 MHz. If achievable, a frequency response such as this would be very attractive for many applications.

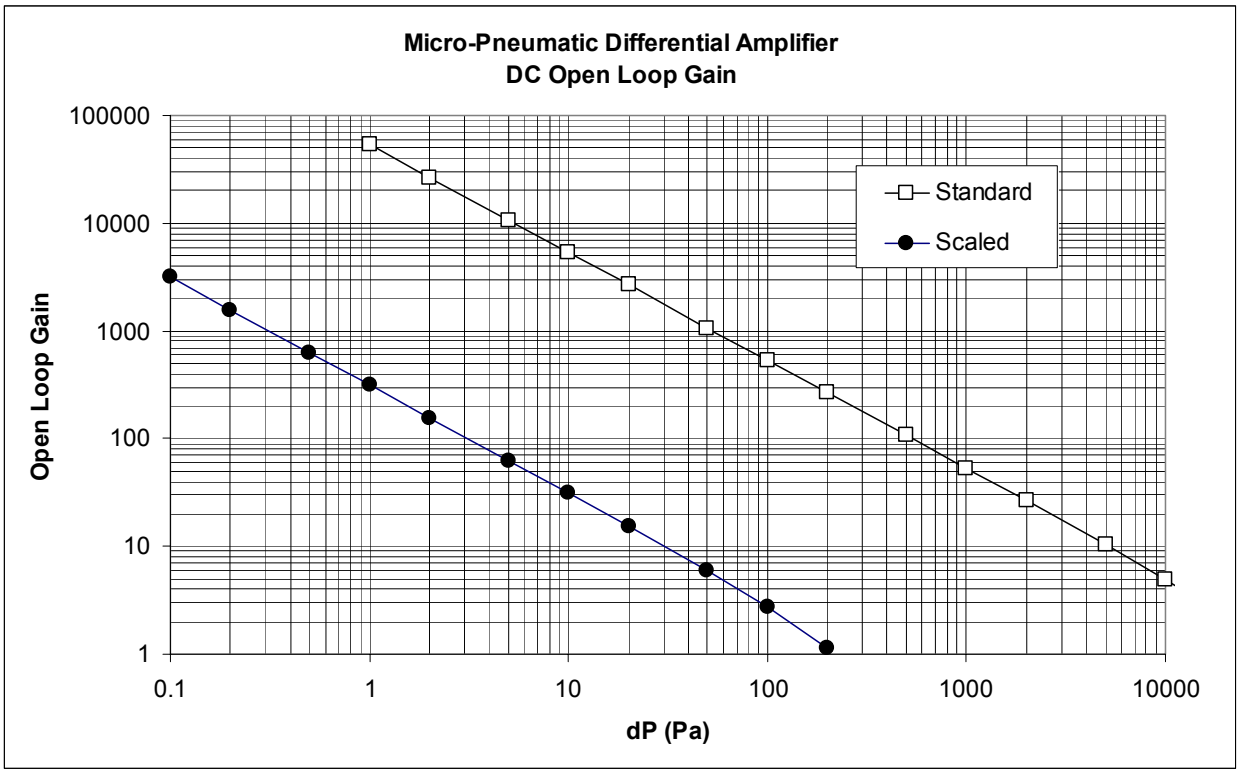

Figure 7: Output for the micro-pneumatic differential operational amplifier of Figure 6, for standard and scaled microvalve technologies. For the simulations resulting in this figure, the pull-up and pull-down devices all have silicon membranes. Standard membranes are 4.5 mm square and 50 µm thick, with a threshold gap of z_0=-6 µm. Scaled membranes are 90 µm square, and 200 nm thick, with a threshold gap of -50 nm. For the standard technology, the pull-up inlet diameter is 85 µm, while the pull-down inlet diameter is 51 µm. For the scaled technology, the pull-up inlet diameter is 8.5 µm, while the pull-down inlet diameter is 5.1 µm. The dimensionless values of A_s and B_s are, respectively, 74.505 and 38.893. For the standard technology, the P_{HI} and P_{LO} pressures are 100,000 and 100 Pa; for the scaled technology, they are 1000 and 10 Pa.

3.2 Mass Pump

In micro-fluidics, it is common for researchers to study pumps, as an active means to propel working fluids through fluidic systems [18, 19]. Using again the analogy to CMOS electronics circuits facilitated by complementary micro-pneumatic devices, however, we find interesting, alternate means for pumping mass through a fluidic system by analyzing CMOS rectifiers.

Figure 8 shows the circuit diagram for a micro-pneumatic full-wave rectifier, based on an analogous CMOS circuit [20]. Power is delivered to the circuit through the oscillating differential pressure source. For purposes of the example depicted in Figures 8 and 9, the oscillation frequency is set to 1 kHz, the center pressure of the oscillator is 50 kPa, and the amplitude of the pressure oscillation is 10 kPa. The diode-like load devices L_1 and L_2 are constructed from the pull-down device of Figure 3, by tying the control and inlet nodes together. All four micro-pneumatic devices have the same design characteristics, except that the diode-like loads have a smaller effective diameter, in order to limit the system losses due to flow through these load devices. Other than the oscillating pressure source, there is no other system 'ground' or power supply. Note that P_0 is at a higher pressure than P_1. Power can be characterized using the relation $\dot{E} = \dot{m}RT$. The power delivered to the load is approximately 25 μW; the total power consumed by all five devices is 105 μW. No attempt to optimize the devices for maximum power delivery to the load has been made.

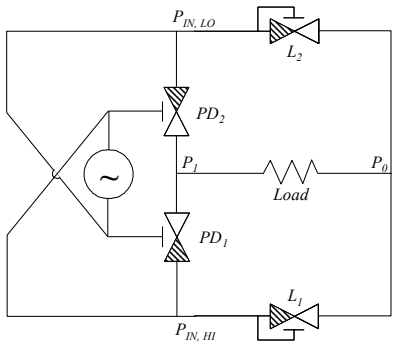

Figure 8: Circuit schematic for a micro-pneumatic full-wave signal rectifier. For the simulations resulting in this figure, the micro-pneumatic valves are all pull-down device as in Figure 3. All have silicon membranes, whose dimensionless values of A_s and B_s are, respectively, 74.505 and 38.893. The membranes are 4.5 mm square and 50 μm thick, with a threshold gap of z_0=-50 nm. The inlet diameters for PD_1 and PD_2 are 85 μm, while for the load devices L_1 and L_2 the inlet diameters are 10 μm. The resistive fluidic load is taken to have a conductance of 10^{-12} kg/Pa-sec. The volumes associated with nodes P_0 and P_1 are taken to be 1 mm^3.

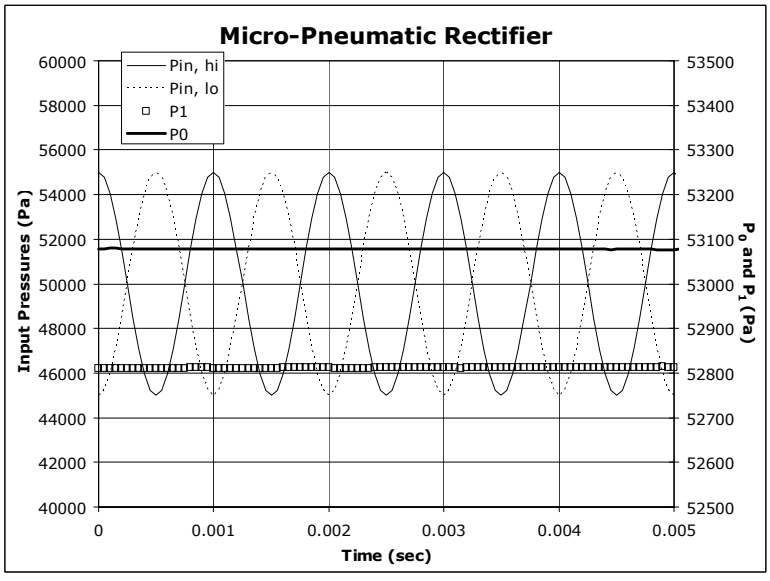

Figure 9: Output for the micro-pneumatic full-wave rectifier of Figure 8.

Figures 10 and 11 repeat the exercise of Figures 8 and 9, with an important exception. As noted earlier, the micro-pneumatic devices of Figures 2 and 3 are not symmetric. Classical CMOS circuit designs employing structures called 'pass gates', however, rely on MOSFET symmetry, in order to achieve the highest circuit performance. In order to realize this symmetry in our micro-pneumatic devices, two devices can be arrayed in parallel, so that flow will be enabled in either direction, given the correct relationships for gate, source, and drain pressures. The schematic based on this concept is seen in Figure 10. The result of applying this circuit to the same conditions as in Figures 8 and 9, is a power efficiency of 27%, but at a much higher differential pressure (3000 Pa vs. 300 Pa). So, increased circuit complexity trades off against higher circuit performance.

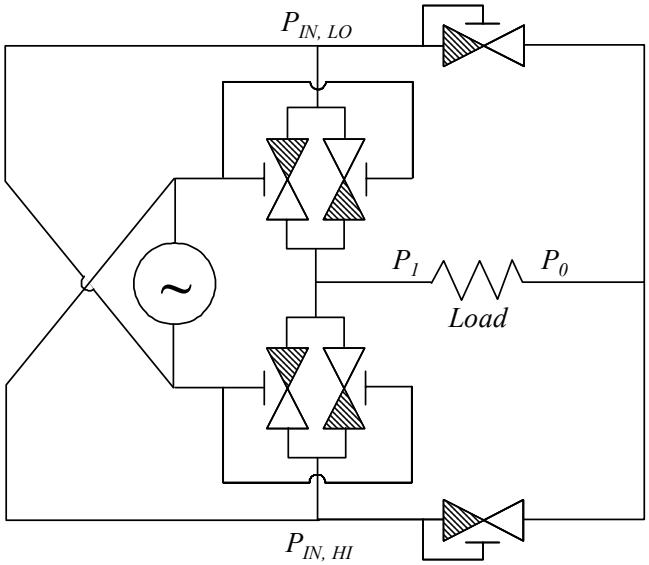

Figure 10: Circuit schematic for a micro-pneumatic full-wave signal rectifier, with fully symmetric pass gates.

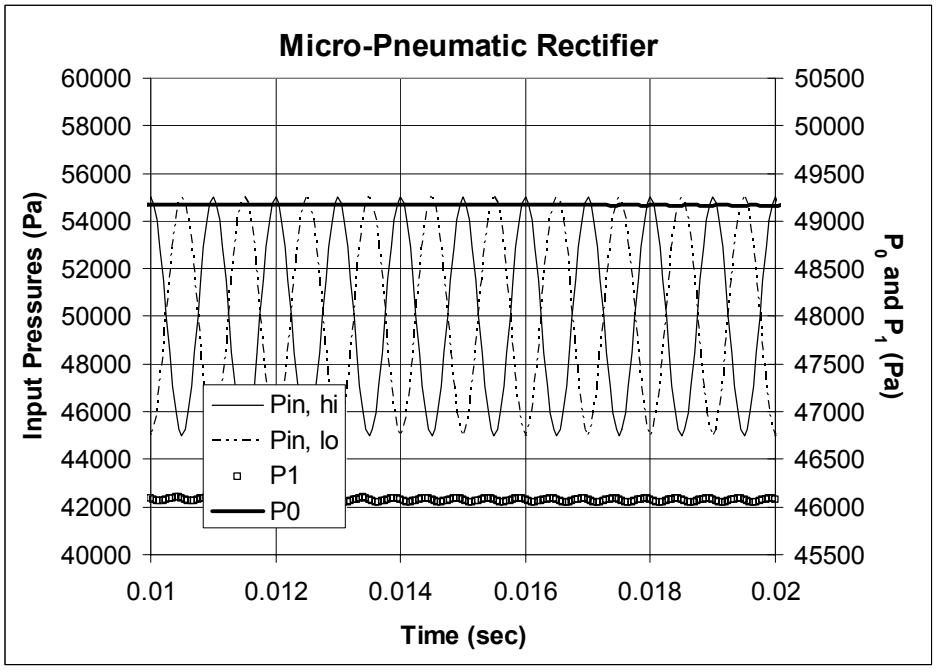

Figure 11: Output for the micro-pneumatic full-wave rectifier with fully symmetric pass gates (see Figure 10).

3.3 Pneumatic Energy Scavenging

With these concepts in mind, we can now explore the application of complementary micro-pneumatic devices to the problem of scavenging energy from pneumatic sources. Figure 12 shows the results of a random pneumatic energy source used as input to the circuit of Figure 10, replacing the previous oscillating source. For this calculation, it is assumed that the random pneumatic energy source has a maximum amplitude of 10 kPa, centered on a value of 50 kPa. Under these assumptions, the power efficiency is in excess of 30%, while the differential pressure across the load has decreased slightly, relative to the well-behaved oscillation for the input studied in Figure 11.

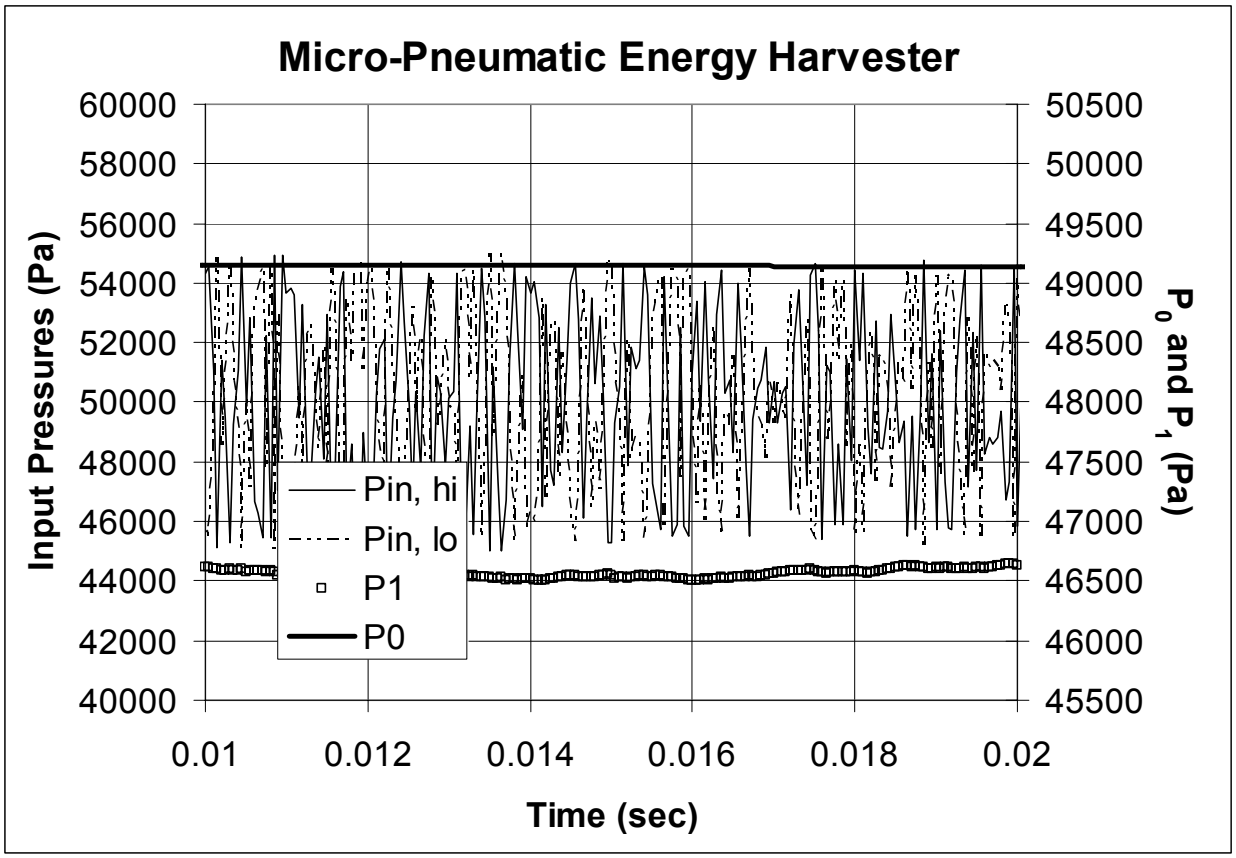

Figure 12: Output for the micro-pneumatic full-wave rectifier with fully symmetric pass gates (see Figure 10), using randomized pressure inputs. The result of this circuit is a relatively efficient conversion of the random pneumatic energy into useful, nearly constant pressure source.

4. DISCUSSION

Extension of the micro-pneumatic technology conceptualized in this work is readily made to fully-complementary micro-*hydraulic* structures, as first presented in Ref. 15. That work recognized the capacitance element in structures controlling incompressible flow must not be fixed-volume elements, as they are when the working fluid is a compressible gas. Rather, for incompressible working fluids, capacitance is realized if one uses a pressure-varying volume to store the incompressible fluid.

The analogy between CMOS electronic information processing systems, and complementary micro-pneumatic systems, reveals a wealth of possibilities for circuits and systems. Further insight into possibilities for pneumatic energy harvesting systems will be gained from examination of CMOS charge pump designs, phase-locked loops, and their integration with current mirrors, operational amplifiers, and simple signal amplifiers.

5. CONCLUSIONS

In this work, application concepts for complementary micro-pneumatic devices and circuits have been presented. In particular, a fundamental building block for analog circuits – the differential operational amplifier – has been designed and studied. A complementary, micro-pneumatic differential op amp based on presently-available technology should demonstrate open loop gains up to 100,000, while consuming 30 sccm of nitrogen at a system inlet pressure of 1 atm, with a cut-off frequency around 1.5 kHz. A scaled technology may deliver comparable open loop gains, with a cut-off frequency of 1.5 MHz, while consuming less than 0.001 sccm of nitrogen for a system inlet pressure of 1000 Pa.

Two types of complementary, micro-pneumatic rectifiers were also studied. In each, full-wave rectification was demonstrated for sinusoidal inputs. Power efficiency of the unoptimized circuits was an acceptable 25-27%. The magnitude of the differential pressure delivered to the load device could be increased nearly ten times, by using a fully symmetric design for the pass gates in the rectifier, instead of a single asymmetric device. The use of complementary micro-pneumatic valves as diodes was also demonstrated. These circuits have direct application as a DC pump derived from an oscillating input pressure.

Finally, the application of these rectifier circuits to the problem of harvesting useful energy from pneumatic systems with randomly varying pressures was studied. The power efficiency of the unoptimized, fully symmetric full-wave rectifier circuit was shown to be in excess of 30%, with useful differential output pressures close the values obtained for well-behaved sinusoidal input pressures.

REFERENCES

1. M. A. Unger, H.-P. Chou, T. Thorsen, A. Scherer, and S. R. Quake, "Monolithic microfabricated valves and pumps by multilayer soft lithography." *Science* **288**, pp. 113-116 (2000).
2. T. Thorsen, S. J. Maerkl, and S. R. Quake, "Microfluidic large-scale integration." *Science* **298**, pp. 580-584 (2002).
3. D. R. Reyes, M. M. Ghanem, G. M. Whitesides, and A. Manz, "Glow discharge in microfluidic chips for visible analog computing," *Lab Chip* **2**(2), pp. 113–116 (2002).
4. M. J. Zdeblick, R. Anderson, J. Jankowski, B. Kline-Schoder, L. Christel, R. Miles, W. Weber, "Thermopneumatically actuated microvalves and integrated electro-fluidic circuits," In *Proceedings, Solid-State Sensor and Actuator Workshop,* pp. 251-255 (1994).
5. S. K. Cho, S. K. Fan, H. Moon, and C.-J. Kim, "Toward digital microfluidic circuits: creating, transporting, cutting and merging liquid droplets by electrowetting-based actuation." In *Proc. 15th Int'l. Conf. MEMS*, pp. 32-35 (IEEE, Piscataway, NJ, 2002).
6. R. B. Fair, V. Srinivasan, H. Ren, P. Paik, V. K. Pamula, and M. G. Pollak, "Electrowetting-based on-chip sample processing for integrated microfluidics." In *Proc. Int'l. Elec. Dev. Mtg.*, pp. 32.5.1-32.5.4 (IEEE, Piscataway, NJ, 2003).
7. W. Zhan and R. M. Crooks, "Microelectrochemical logic circuits." *J. Amer. Chem. Soc.* **125**, pp. 9934-9935 (2003).
8. Z. Hua, Y. Xia, O. Srivannavit, J.-M. Rouillard, X. Zhou, X. Gao, and E. Gulari, "A versatile microreactor platform featuring a chemical-resistant microvalve array for addressable multiplex syntheses and assays." *J. Micromech. Microeng.* **16**, pp. 1433–1443 (2006).
9. H. Takao, M. Ishida, and K. Sawada, "A pneumatically actuated full in-channel microvalve with MOSFET-like function in fluid channel network." *J. Microelectromech.* **11**(5), pp. 421-426 (2002).
10. H. Takao and M. Ishida, "Microfluidic integrated circuits for signal processing using analogous relationship between pneumatic microvalves." *J. Microelectromech.* **12**(4), pp. 497-505 (2003).
11. A. K. Henning, J. S. Fitch, J. M. Harris, E. B. Dehan, B. A. Cozad, L. Christel, Y. Fathi, D. A. Hopkins, Jr., L. J. Lilly, W. McCulley, W. A. Weber, and M. Zdeblick, "Microfluidic MEMS for semiconductor processing." *IEEE Transactions on Components, Packaging, and Manufacturing Technology* **B21**, pp. 329-337 (1998).
12. W. H. Grover, A. M. Skelley, C. N. Liu, E. T. Lagally, and R. A. Mathies, "Monolithic membrane valves and diaphragm pumps for practical large-scale integration into glass microfluidic devices," *Sens. Actuators B, Chem.*, vol. 89, no. 3, pp. 315–323, Apr. 2003.
13. R. A. Mathies, W. H. Grover, B. Paegel, A. Skelley, E. Lagally, C. N. Liu, and R. Blazej, "Fluid control structures in Microfluidic devices." U.S. Patent Application 20040209354 (October 21, 2004).

14. W. H. Grover, R. H. C. Ivester, E. C. Jensen and R. A. Mathies, "Development and multiplexed control of latching pneumatic valves using microfluidic logical structures." *Lab Chip* **6**, pp. 623–631 (2006).
15. A. K. Henning, "Micro-pneumatic logic." In *Proceedings, ASME IMECE 2004*, Paper IMECE2004-61334 (ASME, New York, 2004).
16. A. K. Henning, "Concepts for micropneumatic and microhydraulic logic gates." In *Proceedings, Microfluidic Devices and Systems* (International Society for Optical Engineering, Bellingham, WA, 2007; I. Papautsky, ed.)
17. A. K. Henning, "Compact pressure- and structure-based gas flow model for microvalves." In *Proceedings, Materials and Device Characterization in Micromachining* (International Society for Optical Engineering, Bellingham, WA, 2000; Y. Vladimirsky and P. J. Coane, eds.), volume 4175, pp. 74-81; also, A. K. Henning, "Improved gas flow model for microvalves." In *Proceedings, TRANSDUCERS 2003: 2003 International Solid State Sensors and Actuators Conference*, pp. 1550-1553 (IEEE Press, Piscataway, NJ, 2003).
18. P. Woias, "Micropumps: summarizing the first two decades." In *Proceedings, Microfluidics and BioMEMS* (International Society for Optical Engineering, Bellingham, WA, 2001; C. H. Mastrangelo and H. Becker, eds.), volume 4560, pp. 39-52.
19. D. J. Laser and J. G. Santiago, "A review of micropumps," *J. Micromech. Microeng*. **14**, pp. R35-R64 (2004).
20. H. E. Maleis, "Full-wave rectifier for CMOS IC chip." U.S. Statutory Invention Registration H64 (May 1986).